Optical Fiber Technology 41 (2018) 227–234

Contents lists available at ScienceDirect

Optical Fiber Technology

journal homepage: www.elsevier.com/locate/yofte

Regular Articles

Solution-mediated cladding doping of commercial polymer optical fibers

Pavol Stajanca*, Ievgeniia Topolniak, Samuel Pötschke, Katerina Krebber

Bundesanstalt für Materialforschung und –prüfung (BAM), Unter den Eichen 87, D-12205 Berlin, Germany

ARTICLE INFO

Keywords:
Polymer optical fiber
Solution doping
Polymethyl methacrylate
Rhodamine B
Dye-doped fiber
Fluorescent optical fiber

ABSTRACT

Solution doping of commercial polymethyl methacrylate (PMMA) polymer optical fibers (POFs) is presented as a novel approach for preparation of custom cladding-doped POFs (CD-POFs). The presented method is based on a solution-mediated diffusion of dopant molecules into the fiber cladding upon soaking of POFs in a methanol-dopant solution. The method was tested on three different commercial POFs using Rhodamine B as a fluorescent dopant. The dynamics of the diffusion process was studied in order to optimize the doping procedure in terms of selection of the most suitable POF, doping time and conditions. Using the optimized procedure, longer segment of fluorescent CD-POF was prepared and its performance was characterized. Fiber's potential for sensing and illumination applications was demonstrated and discussed. The proposed method represents a simple and cheap way for fabrication of custom, short to medium length CD-POFs with various dopants.

1. Introduction

In number of applications, polymer optical fibers (POFs) may represent a preferable choice over their silica-based counterparts [1–3]. Polymer materials offer higher chemical flexibility and simpler processing [4,5], which is typically associated with lower POF manufacturing costs. Most common commercial POFs are large-diameter multi-mode (MM) fibers based on polymethyl methacrylate (PMMA). These fibers can be fairly cheap, very robust but flexible, plus they are easy to handle and connectorize [6,7]. Among other advantages, POF technology also allows incorporation of different organic dopants, such as fluorescent dyes, into the fiber material. Fluorescent POFs (F-POFs) have attracted considerable attention in different fields over the years. They have been originally developed in 1980's for scintillation detectors in high energy physics experiments [8,9]. However, since then, F-POFs have been exploited for various tasks in fiber sensing [10], lasing and amplification [11], or illumination [12,13] applications.

Depending on the POF manufacturing procedure, different approaches can be used to incorporate the dopant into the fiber material. Most commonly, the doping is performed on the chemical level, when the dopant is added to the monomer mixture before fiber preform polymerization [14,15]. Alternatively, the dopant can be physically mixed with the polymer melt if the extrusion or casting is used to produce the preform [13]. Finally, solution doping technique has been used to introduce the dopant into the bulk fiber preform [16]. For the vast majority of produced F-POFs, only the core of the fiber is doped. Limited selection of core-doped F-POFs is available also commercially. Cladding doping is in principle possible, however, no cladding-doped POF (CD-POF) is available commercially. Few experimental CD-POFs have been fabricated and explored for different applications. Pun et al. prepared PMMA-based POF with Rhodamine 640-doped cladding and investigated its potential as a side-pumped intrinsic fiber light source [17]. Narro-Garcia et al. fabricated POF with pure PMMA core and THV-Rhodamine 6G cladding for use in illumination applications [12]. Muto et al. used POF with Fluorescein-doped cladding as an optical humidity sensor for breathing condition monitoring [18]. CD-POFs can be of high interest especially in sensing applications. Over the years, numerous fluorescence-based POF sensing schemes have been explored. These include sensors for gamma or UV radiation [19,20], partial discharges [21], humidity [18], position [22], oxygen [23], pH factor [24] and others. Many of these sensing schemes rely on attaching the sensing dye to the side of the fiber. In order to excite and/or collect the light from the dye, some sort of local fiber modification, e.g. tapering, etching or removal and recoating of the cladding, is typically required [20,25]. This sort of local modification usually deteriorates fiber mechanical integrity, increases its loss and offers only limited interaction lengths. Incorporation of the suitable dye directly into the fiber cladding can facilitate efficient interaction between the light propagating inside of the fiber core and the surrounding environment. This could be potentially exploited for construction of various chemical or environmental fiber sensors [26–28].

All of the above-mentioned F-POF manufacturing techniques rely on a doping in a pre-drawing stage. Fabrication of F-POFs in this way, therefore, represents technically demanding process requiring suitable

* Corresponding author.
E-mail addresses: pavol.stajanca@bam.de (P. Stajanca), ievgeniia.topolniak@bam.de (I. Topolniak), samuel.poetschke@bam.de (S. Pötschke), katerina.krebber@bam.de (K. Krebber).

https://doi.org/10.1016/j.yofte.2018.02.008
Received 19 January 2018; Received in revised form 2 February 2018; Accepted 5 February 2018

high-cost equipment and facilities. Recently, solution doping technique was suggested for post-fabrication doping of cladding layer of commercial PMMA POFs [29]. In this work, we present more detailed analysis of solution doping of large-core PMMA POFs as a novel mean for CD-POF fabrication. The technique is studied and optimized in terms of suitable selection of used POF, doping conditions and time. We show that this method may represent rather cheap and straightforward way for preparing custom CD-POFs with short to medium lengths.

2. Doping procedure optimization

POF solution doping technique relies on soaking of a bulk polymer component, e.g. fiber preform, in a suitable solvent-dopant mixture [16]. Successful doping requires selection of the right solvent suitable both for the doped material and the used dopant. In the case of PMMA, methanol is typically used. The technique is commonly employed for doping of microstructured POF preforms either with fluorescent compounds [16,30], or with dopants for increasing fiber photosensitivity [31,32]. The solvent gradually penetrates the bulk polymer and induces its osmotic swelling [33]. At ambient temperatures, ingress of methanol into PMMA exhibits Case II diffusion behavior [34,35], which is characterized by a sharp boundary between the intact inner PMMA region and the swollen outer layer. Due to the solvent-induced swelling, even larger molecules such as organic dyes can diffuse into the PMMA molecular structure. Nevertheless, the mobility of larger dyes is significantly lower than for small solvent molecules and their penetration into the material lags behind the solvent. Similarly as for in-diffusion, also out-diffusion of the solvent is significantly faster than for larger dopant molecules. After the solvent is removed, the dopant molecules are left in the material and their distribution remains stable even at elevated temperatures [30].

Instead of doping bulk polymer elements, we use the solution doping technique directly with commercial PMMA fibers. Various factors such as temperature, specimen geometry or thermal history may influence the diffusion process in PMMA [33,34,36,37]. Therefore, this section is aimed at the basic investigation and optimization of the doping procedure on a small scale, i.e. using short fiber samples and small solvent-dopant mixture quantities.

2.1. Methods and materials

Following the previous studies discussed above, we chose methanol as the suitable doping solvent in this work. LC-MS grade methanol (≥99.95%) from Th. Geyer (Berlin, Germany) was used. The work is focused on the technological aspect of the novel cladding-doping procedure for commercial PMMA POFs. Therefore, we limited this study to using a common and affordable dopant; powdered Rhodamine B (≥95%) from Sigma-Aldrich (Munich, Germany). Nevertheless, we managed to successfully use the presented technique also with several other dopants including Fluorescein, Rhodamine 6G or Alizarin Yellow R. The technique was tested with three different commercial PMMA POFs of similar characteristics; ESKA CK-40 and ESKA GK-40 from Mitsubishi Rayon (Tokyo, Japan) and RAYTELA PGU-FB1000 from Toray (Tokyo, Japan). Some of the main fiber properties extracted from their respective datasheets are listed in Table 1. All the fibers are 1 mm step-index POFs with PMMA core and cladding from perfluorinated polymer.

The doping solution was prepared by dissolving 25 g of Rhodamine B in 75 ml of methanol. This relatively high dopant concentration was chosen in order to facilitate better visibility of the Rhodamine B (RhB) ingress into the fibers. The prepared solution was distributed into multiple small laboratory glass bottles. The tested POFs were cut into short 4 cm pieces. Three fiber pieces were inserted in a bottle with the doping solution, separately for each fiber type. The bottles were closed and stored in a climate chamber at specified temperature for a given time. After the specified time, the samples were taken out of the solution, thoroughly rinsed and dried. The process is schematically illustrated in Fig. 1. The doping procedure was repeated for different doping temperatures and times.

Table 1
Main characteristics of the PMMA POFs used in the study.

	Eska CK-40	Eska GK-40	RAYTELA PGU-FB1000
Fiber diameter [μm]	1000	1000	1000
Core diameter [μm]	980	980	980
Numerical aperture	0.5	0.5	0.5
Operation temperature range [°C]	−55–70	−55–85	−55–70
Transmission loss at 650 nm [dB/km]	≤200	≤150	≤150
Minimum bending radius [mm]	25	20	9

To monitor the lateral ingress of methanol and dye into the fibers, cross-section of the obtained doped samples was investigated with an optical microscope. One end of a doped sample was cut roughly 2 mm away from the original end face. This end of the fiber was inserted in an SMA connector and polished with the help of polishing paper and puck. The connectorized fiber piece was kept in the polishing puck and place on the sample holder of the optical microscope. This helps to keep the fiber in straight upright position so the image of the fiber cross-section can be taken. Inspection of the samples and their cross-sectional images allow us to assess the dynamics of the solvent-dye penetration into the fiber in order to determine the most suitable doping conditions.

2.2. Doping process dynamics

The progress of lateral penetration of methanol-RhB solution into the fiber is illustrated in Fig. 2 for the case of ESKA CK-40 doping at 30 °C. The figure depicts cross-sectional microscope images of the fiber samples that were left in the solution for progressively increasing doping times. The images were taken in the transmitted light mode. Lateral view of each sample is depicted under the corresponding microscope image. The ingress of methanol into the fiber is clearly visible already for the sample with 3 h doping time. The obvious boundary between an intact inner region and a thin swollen outer ring penetrated by methanol can be noticed in the cross-sectional image. As the doping time increases, methanol penetrates deeper into the fiber and the ring gets thicker until the full methanol penetration is reached. The doping series depicted in Fig. 2 serves as an example for illustrating the doping procedure progress. Nevertheless, analogical behavior with different dynamics can be observed for all three tested fibers and different doping temperatures.

To evaluate the progress of methanol front, diameter of the whole fiber D and the inner unpenetrated region d was measured from the microscope images for all the samples. To account for diffusion inhomogeneities, the measurement was performed along four different radial directions. The values were then averaged and used to calculate the relative methanol penetration $P = (D-d)/D$ of the given sample. The final P value of the fiber doped under given conditions was calculated as an average from the three individual fiber samples doped under the same conditions. Fig. 3 shows the time progress of relative methanol penetration into all three tested fibers at 20 °C. We found out that the experimentally measured data (solid points) can be best approximated by a power function fit (solid lines) in a form $P(t) = at^b$. Here, t is the doping time, a and b are the scaling factor and the exponent of the power function, respectively. The power function dependence of $P(t)$ observed in our experiment contradicts previous works [16,34,35]. Methanol ingress into PMMA at ambient temperatures typically exhibits Case II diffusion behavior and the methanol front should progress with a constant velocity. This means that the

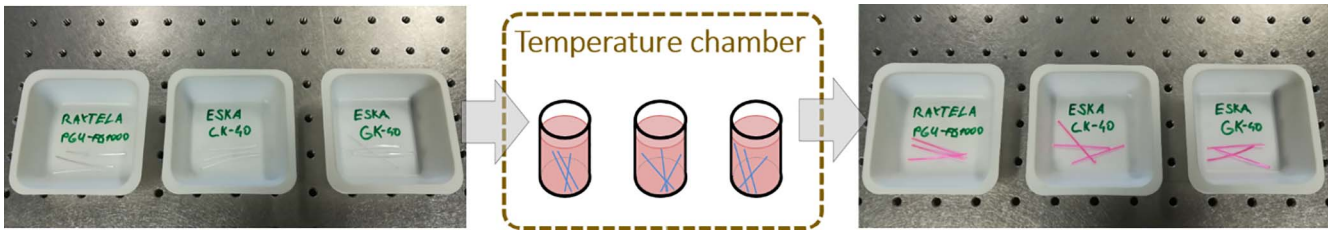

Fig. 1. Schematic illustration of the single doping process used for the doping procedure optimization.

measured $P(t)$ progress should follow a simple linear increase. However, progressive speeding up of diffusion front have been previously observed for spherical and cylindrical samples and can be attributed to radially symmetric geometry [37]. In addition, majority of the previous studies were performed with atactic PMMA samples where no preferential alignment of molecules should be present. This is not the case in our experiment, where PMMA molecules are preferentially align along the fiber axis as a consequence of a fiber heat-drawing. Polymer molecules tend to align along the fiber drawing direction during the manufacturing process. As the fiber cools down, this molecular alignment is "frozen" in the fiber. However, it is a non-equilibrium state and is subject to relaxation (annealing) when the mobility of the molecules is increased, e.g. at elevated temperatures [38] or by presence of the solvents such as methanol [39]. The preferential molecular alignment as well as its simultaneous methanol-induced annealing may influence the basic dynamics of the diffusion process. A deeper analysis of the diffusion process goes beyond the scope of this paper.

Even though the three tested POFs have nominally similar characteristics, Fig. 3 shows that the methanol penetration rate is considerable different for the individual fibers. While doping at 20 °C for 48 h is sufficient to reach full methanol penetration into ESKA GK-40, only roughly 77% and 65% penetration is reached for ESKA CK-40 and RAYTELA fibers at the same conditions, respectively. The time required to reach full methanol penetration t_{full} into the individual fibers can be estimated using the fitted curves. For doping of ESKA GK-40, ESKA CK-40 and RAYTELA POF at 20 °C, approximate t_{full} of 48 h, 60 h and 67 h have been determined, respectively. The differences in penetration dynamics between the fibers most likely stem from the structural differences on the molecular level. Among other parameters [33–37], methanol transport into PMMA is known to be depend on polymer's molecular network structure [36], e.g. degree of crosslinking or entanglement. Although all the fibers are made of PMMA and have very similar geometrical and optical characteristics, the structural organization of PMMA chains may differ considerably between the fibers depending on the particular manufacturing procedure of the individual fibers.

Another factor strongly influencing the doping dynamics is the temperature. The diffusion process is thermally activated and its

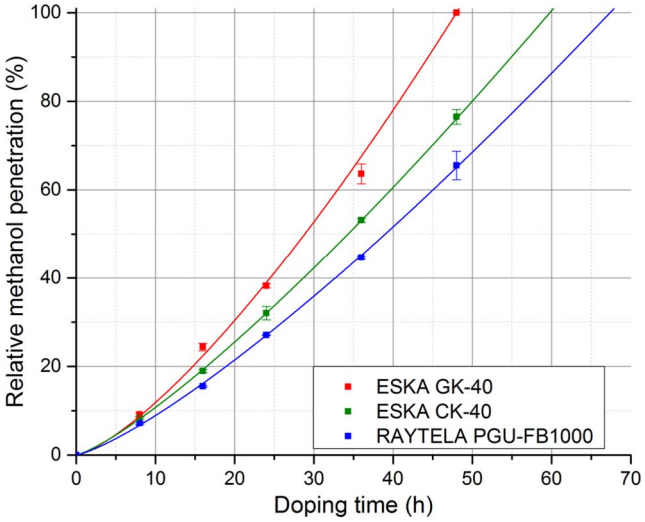

Fig. 3. Relative methanol penetration $P(t)$ into a fiber as a function of doping time t for all three tested POFs at 20 °C. Measured data points are fitted with a power function (solid lines).

temperature dependence is well-known [34,37]. In our case, this is illustrated in Fig. 4 depicting relative methanol penetration into ESKA CK-40 as a function of doping time for different doping temperatures. The rate of methanol penetration into the fiber increases significantly with rising temperature. By increasing the doping temperature by mere 10 °C from 20 °C to 30 °C, almost 4-fold decrease of t_{full} from 60 h to 16 h is achieved. This highlights importance of precise temperature control during the doping. The doping at ambient conditions (without temperature stabilization) is in principle feasible, but would result in deteriorated reproducibility and control over the process.

2.3. Determining optimal doping conditions

So far we focused on the discussion of methanol diffusion into the PMMA POFs. However, the penetration of the dopant dye into the fiber is the key component of the doping process. As expected, penetration of

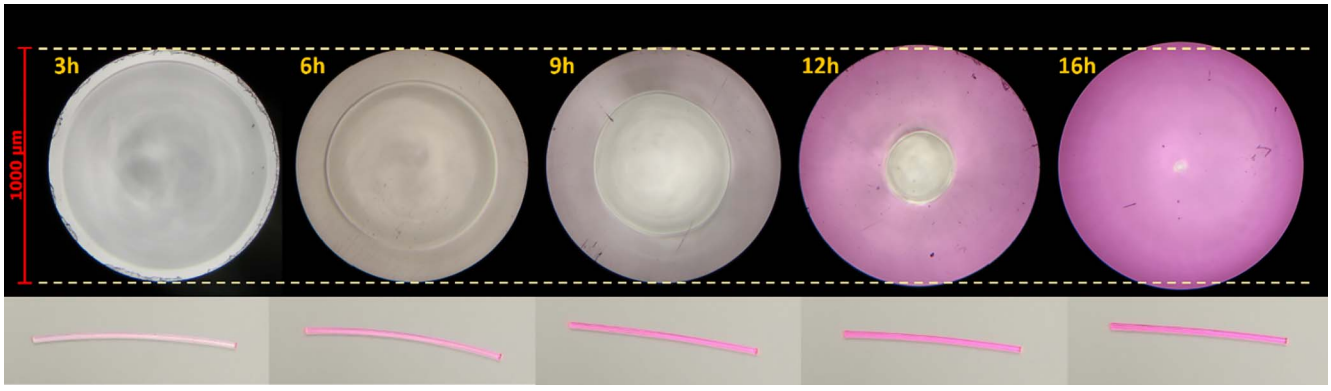

Fig. 2. Cross-sectional and lateral images of ESKA CK-40 samples that were soaked in the doping solution at 30 °C for different times.

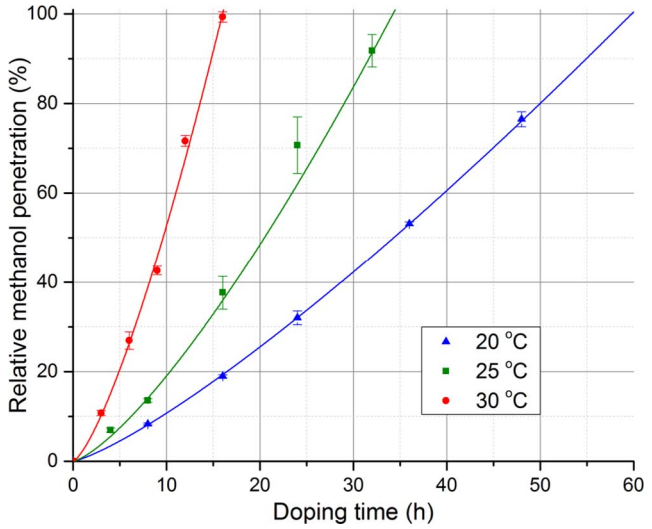

Fig. 4. Relative methanol penetration $P(t)$ into ESKA CK-40 as a function of doping time t for three different doping temperatures. Measured data points are fitted with a power function (solid lines).

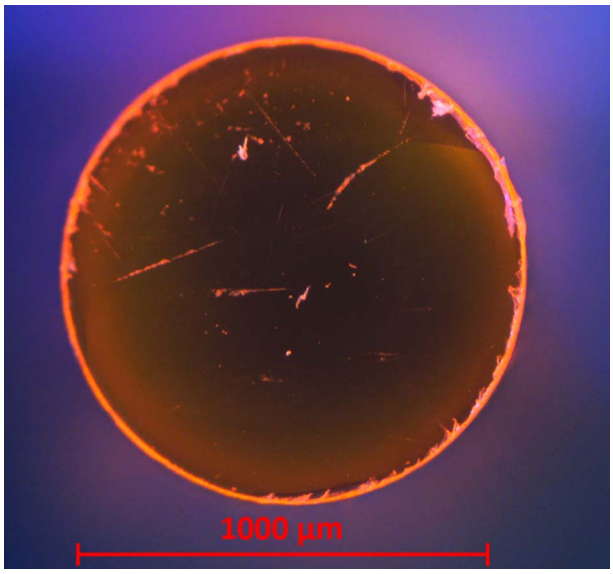

Fig. 5. Microscope image of the cross-section of ESKA CK-40 sample doped for one week at 25 °C. The sample was excited from above by a UV lamp with emission peak around 365 nm.

Rhodamine B into the fiber lacks behind the methanol front significantly. From the lateral photos of the samples in Fig. 2, slightly pinkish color is noticeable already for the sample doped for 3 h. However, RhB most likely diffuses only into outer layer of the fiber cladding. Light coupled into the fiber core is not able to interact with this outer region, therefore, no coloration is observed in the cross-sectional microscope image. Slight coloration of the outer ring penetrated by methanol can be firstly observed for the sample with 9 h doping time. The effect is fully visible for the samples with longer 12 h and 16 h doping times. The outer ring penetrated by methanol appears in a pink/magenta color. This indicates that RhB reached the full penetration of the cladding. The light coupled into the outer ring can interact with RhB at the core-cladding interface. Here, the green part of the white light spectrum is absorbed by RhB molecules, giving rise to observed magenta coloration. Dynamics of the diffusion processes underlying the doping mechanism vary between the tested fibers and doping temperatures. Nevertheless, throughout our study we found consistently that the relative methanol penetration values P between 70% and 80% can be considered a threshold when the full dopant penetration into the fiber cladding is reached.

Interestingly, light in the central unpenetrated region maintains its full (white) spectrum. This indicates that the central region partially guides the light couple into it, i.e. acts as a secondary fiber core. In the first step, this might be explained by lower refractive index (RI) of methanol. Methanol presence effectively decreases RI of the outer ring; thus, giving rise to the secondary core-cladding structure. However, we confirmed that this structure remains visible even for the samples that have been dried at elevated temperatures for extended times. Therefore, the effect is likely caused, at least partially, by permanent reorganization of the PMMA molecular structure induced by methanol presence. Indeed, methanol is known to cause annealing in drawn polymer fibers [39]. Fiber annealing is associated with fiber longitudinal shrinkage and diameter increase. The latter effect can be clearly noticed in Fig. 2, for samples with 12 h and 16 h doping time. Portions of the fibers' cross-section extend beyond the two horizontal guidelines marking the fiber initial diameter. The presented doping method is always accompanied by the fiber annealing.

The secondary core-cladding structure created by methanol-induced annealing is not desirable as it influences the light guiding along the fiber. Therefore, even though shorter times might be sufficient to reach the full dopant penetration into the fiber cladding, only doping times $t \geqslant t_{full}$ providing the full methanol penetration into the fiber will be considered. On the other hand, using doping times much longer than t_{full} is also not optimal. No significant further penetration of RhB into the fiber is observed even for doping times considerably longer than t_{full}. Fig. 5 shows a microscope image of the cross-section of ESKA CK-40 sample that was left in the doping solution for a week at 25 °C. Instead of viewing the sample in transmitted light, like in images in Fig. 2, the sample was excited from above by a handheld LED UV lamp with emission peak around 365 nm. The used doping time is almost five times longer than the determined t_{full} for this fiber at given doping temperature. Despite that, the excited fluorescence is still limited just to the fiber cladding region.

As we discussed earlier, the presented doping procedure is associated with fiber annealing. The degree of the annealing at given temperature increases with the doping time. For long doping times, visible imperfections at the core-cladding interface or even folding of the cladding appear as a result of fiber over-annealing. An extremal case is illustrated in Fig. 6 showing a lateral photo of a 3 cm long sample of ESKA GK-40 doped for 93 h at 20 °C. This is roughly two-times longer than corresponding t_{full} for the fiber. Cladding folds with orientation perpendicular to the fiber axis are clearly visible. Fiber over-annealing and induced imperfections compromise fiber light-guiding and mechanical properties. Therefore, doping times $t \gg t_{full}$ are to be avoided. Over the course of our study, we found out that ESKA GK-40 is the most prone to this effect among the tested POFs. In this case, noticeable degradation of the fiber starts already at $t < t_{full}$ and the fiber is not suitable for the presented doping procedure. On the other hand, ESKA CK-40 was found to be the most tolerant to the effects of over-annealing and we chose it as a default fiber type for the further analysis.

From above discussion, it follows that the progress of methanol

Fig. 6. Lateral photo of the over-annealed 3 cm long ESKA GK-40 sample that was soaked in the doping solution for 93 h at 20 °C.

penetration into the fiber is the decisive factor for determination of optimal doping time t_{opt}. Two competing requirements need to be satisfied simultaneously; On one hand, avoiding presence of the secondary core-cladding structure, which is requiring doping times $t \geqslant t_{full}$. On the other hand, minimizing detrimental effects of fiber annealing, which is asking for doping times as short as possible. Therefore, choosing $t_{opt} = t_{full}$ seems to be ideal. In our case, t_{full} for different fibers and doping conditions has been determined previously using the short samples (Section 2.2). Nevertheless, as can be seen from error bars in Figs. 3 and 4, the rate of methanol penetration into the fiber may vary slightly between the different fiber samples; perhaps because of the local fiber inhomogeneities. When doping longer fiber pieces, using doping times slightly longer than the determined t_{full} helps to assure that the full methanol penetration is achieved all along the sample. As a rule of thumb, we use doping times 10–20% longer than the expected t_{full}.

As we mentioned earlier, microscope study showed that already $t < t_{full}$ are sufficient to reach full dopant penetration into the cladding and facilitate the interaction between the light guided in the fiber core and the dopant. This was true for all three tested fibers and different doping temperatures. Nevertheless, the final concentration of the dopant in the fiber cladding may still depend on number of factors including doping solution concentration, dopant type, temperature as well as doping time. With regard to particular application requirements, further work aimed on the optimization of the dopant concentration and its impact on fiber's optical properties might be required.

3. Fabrication and characterization of CD-POF

Based on the previous analysis and optimization of the doping procedure with short fiber samples, fabrication of longer section of CD-POF is performed and presented in this section. Only results achieved with ESKA CK-40 are presented here as the fiber proved to be the least prone to annealing effects and most suitable for the use with the described doping technique.

3.1. CD-POF fabrication

To perform doping of longer fiber pieces, the proposed doping technique can be relatively easily scaled up by using larger amount of doping solution and glass container. We use the optimized procedure to dope the cladding of a 10 m long piece of ESKA CK-40 with Rhodamine B. The procedure is schematically illustrated in Fig. 7. This time, larger quantity of doping solution was prepared by dissolving 100 mg of RhB in 300 ml of methanol. Note that the concentration of the solution is the same as in optimization study presented in section 2. The fiber was wound into a coil with approximately 20 cm diameter so it can easily fit on the bottom of a glass dish with an inner diameter of 23 cm. The dish was then filled with the doping solution so that the entire fiber is submerged in the solution. The dish was closed with a tight lid and left in the temperature chamber at 20 °C for 68 h. This represents the doping time 8 h longer than the expected t_{full} for this fiber at given temperature. After the doping process, the fiber was removed from the doping solution, thoroughly rinsed and dried. Full methanol penetration into the fiber was verified by microscope inspection of two short pieces cut from the both ends of the doped fiber. The fiber was left to dry; firstly at ambient temperatures for 4 days, followed by additional 2 days at 50 °C. Complete removal of methanol from the fiber was verified by a TGA measurement. For further characterization, the prepared fiber can be easily connectorized with a detachable SMA or ST connectors.

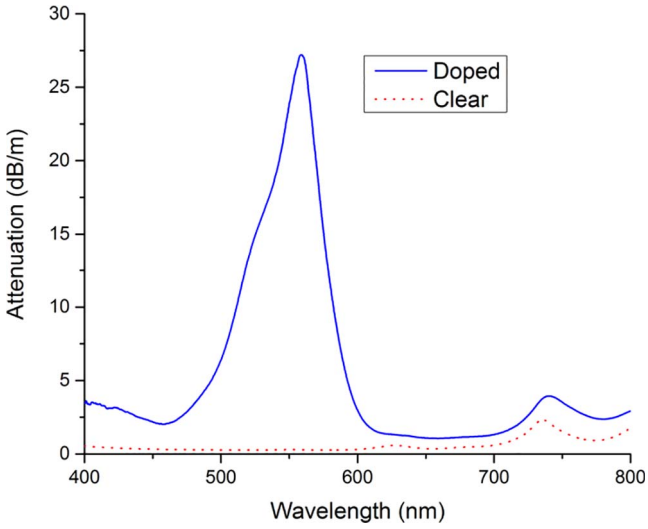

Fig. 8. Spectral attenuation of pristine and RhB-doped ESKA CK-40 POF.

3.2. Fiber attenuation

Fig. 8 compares the attenuation of clear (undoped) and doped ESKA CK-40 measured by the cut-back method. A broadband fiber-coupled Halogen lamp AQ4305 from Yokogawa (Tokyo, Japan) and CCD-based spectrometer HR4000 from Ocean Optics (Largo, FL, USA) were used for the attenuation measurement. In the case of clear POF measurement, initially 10 m long fiber piece was gradually shortened to 1 m in 1 m steps. In the case of doped fiber, 0.5 m long piece was shortened to 0.1 m in 0.1 m steps. Utilization of such a short fiber segment was necessary in order to allow measurement of a high attenuation peak associated with Rhodamine B absorption. The appearance of this absorption peak is clearly visible in Fig. 8 in the green part of the spectrum. The peak has the maximum at 560 nm and a slight shoulder around 520 nm. This is in good agreement with previous works on RhB-doped PMMA POFs [15,40]. Fig. 8 also indicates that the doping procedure increases the fiber overall attenuation in the entire VIS region. From the application point of view, this is especially important in the 600–700 nm spectral window above RhB inherent absorption, where the fiber's fluorescence signals would be located. In this spectral region, cut-back method measurements indicate approximately 3-fold attenuation increase. The measurement was verified by an optical time-domain reflectometry (OTDR) measurement at 650 nm, using multi-

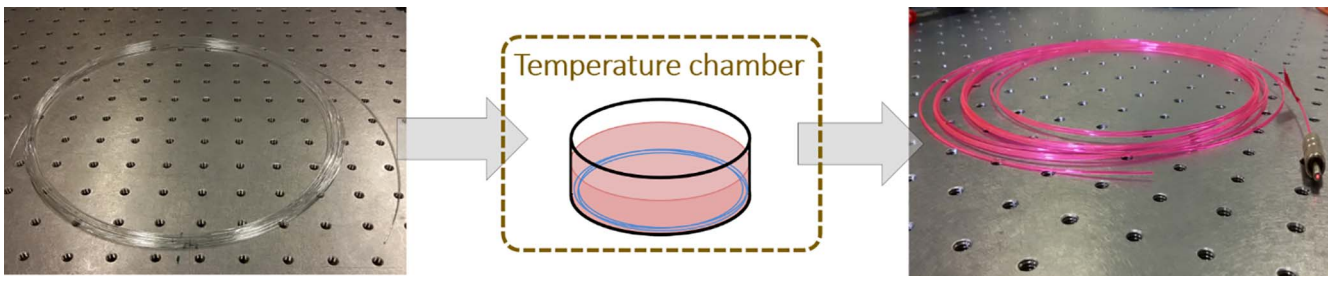

Fig. 7. Schematic illustration of the doping procedure used for preparation of longer CD-POF segments.

mode ν-OTDR from Luciol Instruments (Mies, Switzerland). The OTDR measurement was performed on a 40 m long clear and the 9 m long doped ESKA CK-40 piece. It confirmed roughly 3-fold attenuation increase from 137.8 ± 0.3 dB/km for the clear fiber to 456 ± 4 dB/km for the doped fiber. The observed attenuation increase is most probably caused by the methanol-induced annealing of the fiber that accompanies the doping process.

Despite the attenuation increase, the prepared fiber still performs preferably compared to other experimental CD-POFs fabricated by alternative methods. For PMMA CD-POF with Rhodamine 6G-doped cladding prepared by Narro-Garcia et al., attenuation of about 4.2 dB/m was measured at 633 nm [12]. Another PMMA CD-POF presented by Pun et al. had cladding doped with Rhodamine 640 and exhibited attenuation of 3.129 dB/m at 655 nm [17]. Even though different dopant dyes and concentrations were used in these works, the cited attenuation values were determined at wavelengths well above the absorption bands of the respective dyes. Therefore, similarly as in our case, light absorption by the dopant should not contribute significantly to the measured attenuation. The both stated attenuation levels are considerably higher than for our CD-POF at comparable wavelengths (~ 0.5 dB/m). The achieved attenuation should be sufficient for sensing or lighting applications using fibers with several meter length range.

3.3. Fiber fluorescence properties

Fluorescence properties of the prepared CD-POF were investigated using side-illumination technique [41,42], with the help of setup schematically depicted in Fig. 9. One end of the prepared CD-POF piece was connectorized with an SMA connector and connected to the same spectrometer as used for fiber attenuation measurement (Section 3.2). Halogen lamp (also described in section 3.2) was coupled to a 2 long clear POF cable. The white light exiting the other end of the POF cable was used to laterally excite the CD-POF at different positions along the fiber. For each excitation position, output end of the lead-in POF cable was brought into direct physical contact in perpendicular direction with the CD-POF. The excited fluorescence from the fiber cladding is partially coupled to the fiber core and guided towards the spectrometer where it is measured. The experiment was performed in a dark room to avoid parasitic fluorescence excitation by surrounding light.

Ideally, monochromatic light source with wavelength corresponding to the dye absorption peak should be used for the side-illumination experiments [41,42]. Due to the lack of such a light source with sufficient temporal stability, we decided to use the halogen lamp. The lamp provides very stable broadband emission covering VIS and NIR wavelengths. To verify validity of our approach, the spectra obtained by the white-light excitation were compared to the ones obtained using the narrowband UV LED lamp (365 nm) at the same excitation positions along the fiber. Except of higher absolute intensities in the case of UV excitation, the spectra were practically identical. However, the UV lamp output fluctuates considerably and the lamp is therefore not suitable for the side-illumination measurement. The comparison confirms the validity of our experimental approach. Fig. 10 shows the evolution of measured fluorescence spectrum as the excitation position was moved away from the CD-POF output end connected to the spectrometer. The spectrum obtained under UV excitation at the shortest excitation distance (0.1 m) is included for comparison.

Fig. 9. Schematic illustration of the experimental setup used for the CD-POF side-illumination fluorescence measurement.

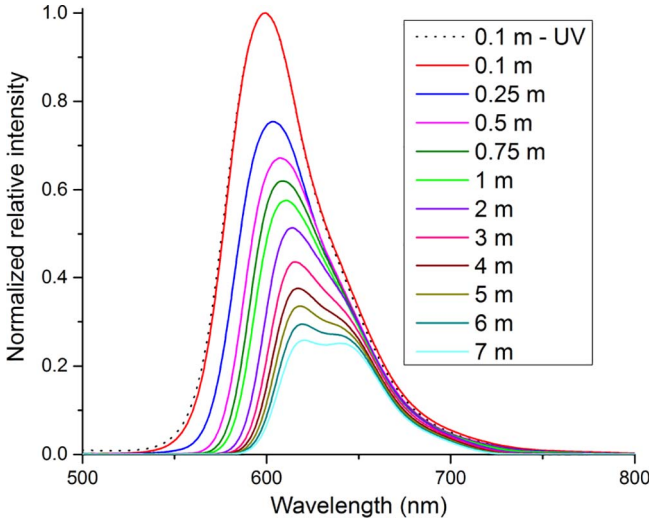

Fig. 10. Fluorescence spectrum registered from the CD-POF core under fiber side excitation by a white light as the excitation position was moved away from the monitoring end. The spectrum obtained under UV excitation at the shortest excitation distance (0.1 m) is included for comparison.

As the excitation position moves away from the CD-POF monitoring end, the intensity of recorded fluorescence drops considerably and its peak emission wavelength shifts toward the longer wavelengths. Fig. 11 depicts the fluorescence normalized relative integral intensity and peak wavelength as a function of excitation position evaluated from the spectra depicted in Fig. 10. The figure shows that the intensity and peak wavelength change is most significant at the short excitation distances. This effect is common for all fluorescent fibers and is predominantly caused by a strong fluorescence reabsorption by the dopant dye molecules. At the excitation point, part of the broadband fluoresce of Rhodamine B, with peak emission around 575 nm [15,40], is coupled into the fiber core where it propagates further. As it propagates along the fiber, part of the light is reabsorbed by RhB molecules at the core-cladding interface. The shorter wavelengths with larger overlap with RhB absorption peak are absorbed faster. This is responsible for an abrupt attenuation and red-shift of the florescence spectra observed on the short propagation distances. As the propagation continues, lower wavelengths overlapping dopant absorption spectrum are gradually completely attenuated and further spectrum evolution is predominantly dictated by fiber inherent attenuation. The effect can be used for characterization of fluorescent fibers [41,42], but has been also exploited directly for sensing applications, e.g. linear position measurement [22]. The setup can be used as a contactless position and movement sensor along the fiber. In our case, the fluorescence can be easily detected even for excitation 7 m away from the monitoring end. The decrease of fluorescence integral intensity between excitation at 0.1 m and 7 m from the detector is at the level of 6 dB. The results illustrates fiber's ability to collect and guide the fluorescence from the cladding over extended distances. This is important for number of applications relying on the side-excitation scheme [17,20–22].

CD-POFs may be used also for illumination applications [12,43]. In this case, in-core pumping by light with wavelength within dopant absorption spectrum is used. As the pump light propagates through the fiber it interacts with the dopant at the core-cladding interface and excites its fluorescence. Fig. 12 shows an image of the prepared 9 m long CD-POF under in-core pumping with 365 nm UV light from the LED lamp. Fiber visibly glows with orange fluorescence of Rhodamine B. The intensity of the fluorescence decreases along the fiber due to the gradual pump light depletion. Fiber pumping from both ends is typically used to mitigate this effect and achieve more homogeneous illumination. The results illustrate potential of CD-POFs prepared by our

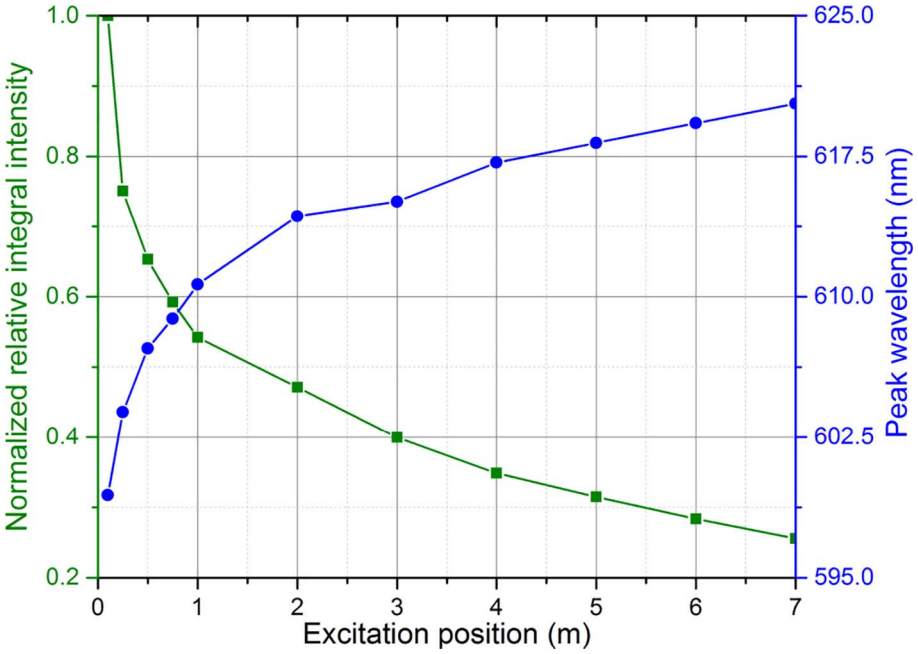

Fig. 11. Fluorescence normalized relative integral intensity and peak wavelength as a function of excitation position along the fiber.

novel technique for lighting applications. Fiber glow color can be altered by using different fluorescent dopants (Fig. 12: Inlay). Although the presented study is limited to the use of RhB as the fiber dopant, we have successfully used the doping technique also with other fluorescent dyes, such as Rhodamine 6G or Fluorescein.

4. Summary and conclusions

In this work, a novel method for preparation of cladding-doped POFs based on solution doping of commercial PMMA fibers is presented. The solution doping technique relies on the diffusion of dopant into the cladding of POF upon its soaking in methanol-dopant solution. The first part of the work was focused on the technological aspect of the doping process with an aim of finding most suitable procedure. The doping technique was tested with three different 1 mm commercial PMMA POFs; ESKA CK-40 and ESKA GK-40 from Mitsubishi Rayon (Tokyo, Japan) and RAYTELA PGU-FB1000 from Toray (Tokyo, Japan). ESKA GK-40 was deemed unsuitable for the proposed technique as it suffers from the significant methanol-induced annealing which degrades fiber optical and mechanical performance. On the other hand, ESKA CK-40 was found as the most suitable from the tested fibers because it is least prone to the annealing effects. This fiber was used for the rest of the study. Nevertheless, reasonable results might be achieved also with RAYTELA PGU-FB1000 under optimized doping conditions.

The results indicate that selection of optimal doping time is dictated predominantly by progress of methanol diffusion into the fiber. Too short doping times lead to creation of undesirable secondary core-cladding structure and might not be sufficient for dopant to reach full penetration into the fiber cladding (Fig. 2). In Contrast, too long doping times lead to fiber over-annealing and degradation of its optical and mechanical properties (Fig. 5). Therefore, dynamics of methanol diffusion into the fibers was measured under different conditions. Strong temperature dependence of methanol penetration into the fiber was found (Fig. 4). This pinpoints importance of doping temperature control. Shortest doping time guaranteeing full methanol penetration into the fiber was found optimal for the proposed procedure.

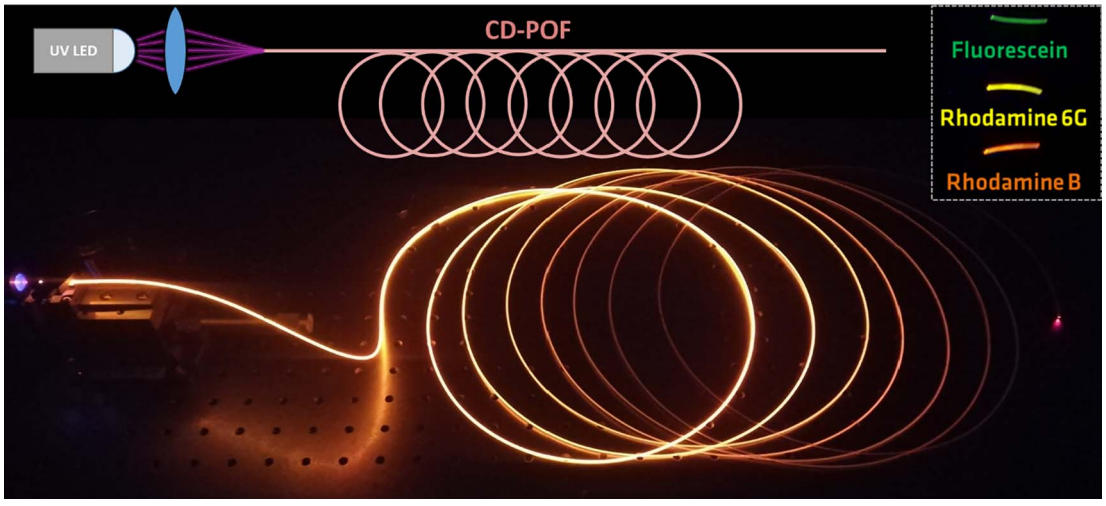

Fig. 12. Photo of lateral emission of the 9 m long CD-POF under in-core excitation with 365 nm UV light. Inlay: Photo of short segments of CD-POFs doped with different dyes under side-excitation by the UV light.

Based on performed optimization of the process, 10 m long CD-POF with Rhodamine B-doped cladding was prepared and characterized in the second part of the work. Fiber attenuation measurement (Fig. 8) confirmed that RhB was successfully incorporated into the fiber cladding in a way that the dye can interact with the light propagating in the fiber core. The measurement also showed that, due to methanol-induced annealing, the doping process generally increased fiber attenuation by factor of three even at wavelengths outside RhB absorption spectrum. Despite this increase, fiber's attenuation properties might be considered better than for other CD-POFs prepared by alternative methods [12,17], and sufficient for applications with meter-long fiber range. Using side-illumination technique, we demonstrated fiber's ability to efficiently collect and monitor dopant fluorescence over extended fiber lengths (Fig. 10). CD-POFs prepared by the proposed technique might be, therefore, especially interesting for number of sensing applications relying on side-excitation or evanescent field sensing. Environmental sensing applications are particularly attractive since a POF with suitably doped cladding can facilitate efficient interaction between the light propagating in the fiber core and fiber surroundings. At the same time, we illustrated potential of the CD-POF for illumination applications under in-core pumping configuration (Fig. 12).

The proposed procedure represents a novel, simple and cost-effective way for preparing cladding-doped POFs with short to medium lengths. With exception of the climate chamber, which can be switched for a simpler temperature oven, no specialty high-cost equipment was necessary for the CD-POF preparation. Although the work presented in this paper focuses predominantly on doping with Rhodamine B, we successfully tested the procedure also with several other dyes. The technique should be readily adaptable for use with variety of other dopants, although, further optimization might be required in certain cases. The proposed method is not to be viewed as a substitute/competition for more traditional fabrication techniques, based on doping in the pre-drawing stage, for large scale production of already optimized CD-POFs. However, the method can be very useful as a simple and cheap CD-POF fabrication technique for initial optimization and validation tasks, especially at the research facilities that do not possess specialty preform and fiber manufacturing equipment.

Acknowledgement

The research leading to these results has received funding from the People Programme (Marie Curie Actions) of the European Union's Seventh Framework Programme FP7/2007 2013/ under REA grant agreement n° 608382.

References

[1] M. Plümpe, M. Beckers, V. Mecnika, G. Seide, T. Gries, C.-A. Bunge, 9 - Applications of polymer-optical fibres in sensor technology, lighting and further applications, in: C.-A. Bunge, T. Gries, M. Beckers (Eds.), Polymer Optical Fibres: Fibre Types, Materials, Fabrication, Characterisation and Applications, Woodhead Publishing, 978-0-08-100039-7, 2017.
[2] I. Tafur Monroy, H.P.A. vd Boom, A.M.J. Koonen, G.D. Khoe, Y. Watanabe, Y. Koike, T. Ishigure, Data transmission over polymer optical fibers, Opt. Fiber Technol. 9 (2003) 159–171.
[3] K. Peters, Polymer optical fiber sensors – a review, Smart Mater. Struct. 20 (2011) 013002.
[4] M. Beckers, T. Schlüter, T. Gries, G. Seide, C.-A. Bunge, 6 - Fabrication techniques for polymer optical fibres, in: C.-A. Bunge, T. Gries, M. Beckers (Eds.), Polymer Optical Fibres: Fibre Types, Materials, Fabrication, Characterisation and Applications, Woodhead Publishing, 978-0-08-100039-7, 2017.
[5] M. Beckers, T. Schlüter, T. Vad, T. Gries, C.-A. Bunge, An overview on fabrication methods for polymer optical fibers, Polym. Int. 64 (2015) 25–36.
[6] O. Ziemann, J. Krauser, P.E. Zamzow, W. Daum, P.O.F. Handbook, Optical Short Range Transmission Systems, 2nd ed., Springer, Berlin, 978-3-540-76628-5, 2008.
[7] Y. Koike, Fundamentals of Plastic Optical Fibers, Wiley, Weinheim, 978-3-527-41006-4, 2015.
[8] H. Blumenfeld, M. Bourdinaud, J.C. Thevenin, Plastic fibers in high energy physics, Nucl. Instr. Meth. Phys. Res. A 257 (1987) 603–606.
[9] H. Blumenfeld, M. Bourdinaud, J.C. Thevenin, Scintillating plastic fibres for calorimetry and tracking devices, IEEE Trans. Nucl. Sci. 33 (1986) 54–56.
[10] R.J. Barlett, R. Philip-Chandy, P. Eldridge, D.F. Merchant, R. Morgan, P. Scully, Plastic optical fibre sensors and devices, Trans. Inst. Meas. Control 22 (2000) 431–457.
[11] J. Arrue, F. Jimenez, I. Ayesta, M.A. Illarramendi, J. Zubia, Polymer-optical-fiber lasers and amplifiers doped with organic dyes, Polymers 3 (2011) 1162–1180.
[12] R. Narro-Garcia, R. Quintero-Torres, J.L. Dominguez-Juarez, M.A. Ocampo, Polymer optical fiber with Rhodamine doped cladding for fiber light systems, J. Lumin. 169 (2016) 295–300.
[13] I. Parola, E. Arrospide, F. Recart, A.M. Illarramendi, G. Durana, N. Guarrotxena, O. García, J. Zubia, Fabrication and characterization of polymer optical fibers doped with perylene-derivatives for fluorescent lighting applications, Fibers 5 (2017).
[14] P.H. Rebourgeard, F. Rondeaux, J.P. Baton, G. Besnard, H. Blumenfeld, M. Bourdinaud, J. Calvet, J.C. Cavan, R. Chipaux, A. Giganon, J. Heitzmann, C. Jeanney, P. Micolon, M. Neveu, T. Pedrol, D. Pierrepont, J.C. Thevenin, Fabrication and measurement of plastic scintillating fibers, Nucl. Instr. Meth. Phys. Res. A 427 (1999) 543–567.
[15] H. Liang, Z. Zheng, Z. Li, J. Xu, B. Chen, H. Zhao, Q. Zhang, H. Ming, Fabrication and amplification of Rhodamine B-doped step-index polymer optical fiber, J. Appl. Polym. Sci. 93 (2004) 681–685.
[16] M.C.J. Large, S. Ponrathnam, A. Argyros, N.S. Pujari, F. Cox, Solution doping of microstructured polymer optical fibres, Opt. Express 12 (2004) 1966–1971.
[17] C.F.J. Pun, Z. Liu, M.L.V. Tse, X. Cheng, X.M. Tao, H.Y. Tam, Side-illumination fluorescence dye-doped-clad PMMA-core polymer optical fiber: potential intrinsic light source for biosensing, IEEE Phot. Technol. Lett. 24 (2012) 960–962.
[18] S. Muto, H. Sato, T. Hosaka, Optical humidity sensor using fluorescent plastic fiber and its application to breathing-condition monitor, Jpn. J. Appl. Phys. 33 (1994) 6060–6064.
[19] W.B. Lyons, C. Fitzpatrick, C. Flanagan, E. Lewis, A novel multipoint luminescent coated ultra violet fibre sensor utilising artificial neural network pattern recognition techniques, Sens. Actuators A-Phys. 115 (2004) 267–272.
[20] C. Fitzpatrick, C. O'Donoghue, E. Lewis, A novel multi-point ultraviolet optical fibre sensor based on cladding luminescence, Meas. Sci. Technol. 14 (2003) 1477–1483.
[21] D. Siebler, P. Rohwetter, R. Brusenbach, R. Plath, Optical-only detection of partial discharge with fluorescent polymer optical fiber sensors, Procedia Eng. 120 (2015) 845–848.
[22] P. Aiestaran, V. Dominguez, J. Arrue, J. Zubia, A fluorescent linear optical fiber position sensor, Opti. Mater. 31 (2009) 1101–1104.
[23] M. Morisawa, S. Muto, POF sensors for detecting oxygen in air and water, 7th International Plastic Optical Fibres Conference '98, Berlin, Germany, 1998, pp. 243–244.
[24] X.H. Yang, L.L. Wang, Fluorescence pH probe based on microstructured polymer optical fiber, Opt. Express 15 (2007) 16478–16483.
[25] C. Pulido, O. Esteban, Improved fluorescence signal with tapered polymer optical fibers under side-illumination, Sens. Actuators B-Chem. 146 (2010) 190–194.
[26] R.A. Potyrailo, G.M. Hieftje, Distributed fiber-optic chemical sensor with chemically modified plastic cladding, Appl. Spectrosc. 52 (1998) 1092–1095.
[27] R.A. Potyrailo, G.M. Hieftje, Oxygen detection by Fuorescence quenching of tetraphenylporphyrin immobilized in the original cladding of an optical fiber, Anal. Chim. Acta 370 (1998) 1–8.
[28] R.A. Potyrailo, G.M. Hieftje, Optical time-of-flight chemical detection: spatially resolved analyte mapping with extended-length continuous chemically modified optical fibers, Anal. Chem. 70 (1998) 1453–1461.
[29] P. Stajanca, K. Krebber, Post-fabrication cladding doping of commercial PMMA polymer optical fiber. in: R. Nogueira, A.M. Rocha (Eds.), 26th International Conference on Plastic Optical Fibres, Aveiro, Portugal, 2017, p. 14.
[30] A. Argyros, M.A. van Eijkelenborg, S.D. Jackson, R.P. Mildren, Microstructured polymer fiber laser, Opt. Lett. 29 (2004) 1882–1884.
[31] X. Hu, G. Woyessa, D. Kinet, J. Janting, K. Nielsen, O. Bang, C. Caucheteur, BDK-doped core microstructured PMMA optical fiber for effective Bragg grating photoinscription, Opt. Lett. 42 (2017) 2209–2212.
[32] D. Sáez-Rodríguez, K. Nielsen, H.K. Rasmussen, O. Bang, D.J. Webb, Highly photosensitive polymethyl methacrylate microstructured polymer optical fiber with doped core, Opt. Lett. 38 (2013) 3769–3772.
[33] N.L. Thomas, A.H. Windle, A deformation model for Case II diffusion, Polymer 21 (1980) 613–619.
[34] N.L. Thomas, A.H. Windle, Transport of methanol in poly(methyl methacrylate), Polymer 19 (1978) 255–265.
[35] J. Muto, S. Tajika, Diffusion of alcohol-rhodamine 6G in polymethyl methacrylate, J. Mate. Sci. 21 (1986) 2114–2118.
[36] A.K. Ekenseair, N.A. Peppas, Network structure and methanol transport dynamics in poly(methyl methacrylate), AIChE J. 58 (2012) 1600–1609.
[37] P.I. Lee, Temperature dependence of methanol transport in spherical PMMA beads, Polymer 34 (1993) 2397–2400.
[38] P. Stajanca, O. Cetinkaya, M. Schukar, P. Mergo, D.J. Webb, K. Krebber, Molecular alignment relaxation in polymer optical fibers for sensing applications, Opt. Fiber Technol. 28 (2016) 11–17.
[39] A. Fasano, G. Woyessa, J. Janting, H.K. Rasmussen, O. Bang, Solution-mediated annealing of polymer optical fiber bragg gratings at room temperature, IEEE Phot. Technol. Lett. 29 (2017) 687–690.
[40] A. Tagaya, Y. Koike, T. Kinoshita, E. Nihei, T. Yamamoto, K. Sasaki, Polymer optical fiber amplifier, Appl. Phys. Lett. 63 (1993) 883–884.
[41] R.J. Kruhlak, M.G. Kuzyk, Side-illumination fluorescence spectroscopy. II. Applications to squaraine-dye-doped polymer optical fibers, J. Opt. Soc. Am. B 16 (1999) 1756–1767.
[42] R.J. Kruhlak, M.G. Kuzyk, Side-illumination fluorescence spectroscopy. I. Principles, J. Opt. Soc. Am. B 16 (1999) 1749–1755.
[43] L. Jaramillo-Ochoa, R. Narro-García, M.A. Ocampo, R. Quintero-Torres, High stability of polymer optical fiber with dye doped cladding for illumination systems, J. Lumin. 184 (2017) 205–210.